Copolymers of Cyclopentadithiophene and Electron-Deficient Aromatic Units Designed for Photovoltaic Applications

By *Johan C. Bijleveld, Munazza Shahid, Jan Gilot, Martijn M. Wienk,* and *René A. J. Janssen**

Alternating copolymers based on cyclopentadithiophene (CPDT) and five different electron-deficient aromatic units with reduced optical band gaps are synthesized via Suzuki coupling. All polymers show a significant photovoltaic response when mixed with a fullerene acceptor. The frontier orbital levels of the new polymers are designed to minimize energy losses by increasing the open-circuit voltage with respect to the optical band gap, while maintaining a high coverage of the absorption with the solar spectrum. The best cells are obtained for a copolymer of CPDT and benzooxadiazole (BO) with a band gap of 1.47 eV. This cell gives a short-circuit current of 5.4 mA cm^{-2}, an open-circuit voltage of 0.78 V, and a fill factor of 0.6, resulting in a power conversion efficiency of about 2.5%.

1. Introduction

Thin-film bulk-heterojunction polymer solar cells offer an opportunity for low-cost renewable energy production. These devices use a phase-separated blend of two organic semiconductors with offset energy levels that lead to an intermolecular charge transfer between the two components after photoexcitation.[1] Blends of conjugated polymers as donor and fullerene derivatives as acceptor have emerged as a very successful combination. The power conversion efficiency of these devices depends on the quantum and energy efficiency by which photons from the sun can be converted into charges in an external circuit. To be efficient, absorption of light as well as charge generation, transport, and collection all have to occur with high quantum efficiency (i.e., converting all photons into electrons) and with minimal losses in energy (i.e., keeping the photovoltage close to the photon energy). The complex sequence of events is controlled by several materials and device parameters of which optical absorption, relative position of energy levels, charge carrier mobility, and nanoscale morphology are probably most important. The power conversion efficiency of these devices has recently reached levels close to 6% in single junctions.[2,3]

New materials that are able to convert a larger fraction of the solar spectrum have contributed significantly to improving the energy conversion efficiency.[2,4–14] The main strategy to control the band gap of conjugated polymers is incorporating electron-rich (donors) and electron-poor groups (acceptors) in an alternating fashion in the main chain of the polymer.[15] The energy conversion efficiency of a photovoltaic cell is set by the product of short-circuit current density (J_{sc}), fill factor (FF), and open-circuit voltage (V_{oc}) relative to the light intensity. Design rules for electron donor and acceptor materials with maximum performance have been outlined by Scharber et al.[16] and here we follow a similar approach. We assume that the energy levels of the highest occupied molecular orbital (HOMO) and lowest unoccupied molecular orbital (LUMO) for the donor:acceptor blend are as shown in Figure 1a. Within this

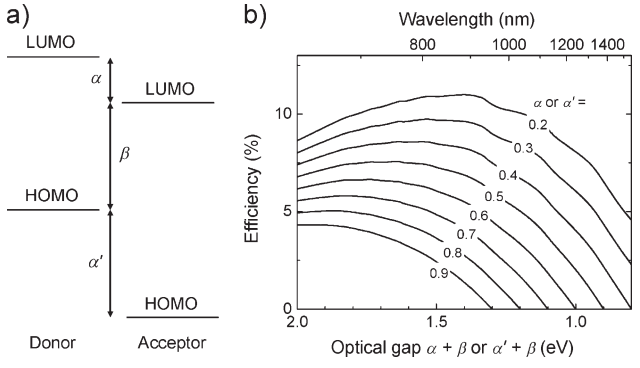

Figure 1. a) Simplified presentation of the frontier orbital energy levels in a bulk-heterojunction solar cell, defining the offset energies α, α', and β. b) AM1.5G energy conversion efficiency of bulk-heterojunction solar cells as function of α (or α') and β, assuming that EQE = 0. 65 for energies larger that the optical gap, FF = 0.65, and $eV_{oc} = \beta - 0.4$ eV.

[*] Prof. R. A. J. Janssen, J. C. Bijleveld, Dr. M. Shahid, J. Gilot, Dr. M. M. Wienk
Molecular Materials and Nanosystems
Eindhoven University of Technology
P.O. Box 513
5600 MB Eindhoven (The Netherlands)
E-mail: r.a.j.janssen@tue.nl
Dr. M. Shahid
Dutch Polymer Institute (DPI)
P.O. Box 902
5600 AX Eindhoven (The Netherlands)

DOI: 10.1002/adfm.200900412

approximation, photoinduced charge transfer will occur if there is a net gain in energy α (or α') for electron (or hole) transfer upon excitation of the donor (or acceptor). Note that α (or α') actually represents an energy loss in the operation of the device. The open-circuit voltage of a bulk heterojunction solar cell is related to energy difference β between the HOMO of the electron donor and the LUMO of the acceptor.[4,17–19] In practice, the actual value is about 0.4 V less than β.[18] The smallest optical gap of donor ($\alpha + \beta$) or acceptor ($\alpha' + \beta$) determines the onset of absorption of the materials. Within this simplified energy level diagram it is then straightforward to estimate maximum energy conversion efficiency of an organic donor:acceptor solar cell with α (or α') as a parameter by integrating photons of the AM1.5G spectrum above the optical gap $\alpha + \beta$ (or $\alpha' + \beta$) that are absorbed and assigning them an energy equal to $\beta - 0.4$ eV. The diagram in Figure 1b is created by arbitrarily assuming a FF = 0.65 and an external quantum efficiency (EQE) of 0.65 over the whole absorption range.[20] Figure 1b clearly identifies α (or α') as a crucial parameter and shows that ultimately the efficiency drops at low and high values of the optical gap because of a loss in voltage or a loss in current, respectively. In general it is assumed that a substantial offset α (or α') = 0.3–0.4 eV[21–23] is required to provide quantitative charge transfer, which would place the optimum band gap of conjugated polymers for bulk heterojunction solar cells in a broad range between 1.35 and 1.8 eV. Figure 1b can also be used to gauge the potential power conversion efficiency for any donor:acceptor materials combination when α, α', and β are known.

One of the best bulk heterojunction solar cells up to now, with a reported power conversion efficiency of $\eta = 5.5\%$,[2] has an active layer that consists of poly(4,4-di(2-ethylhexyl)-4*H*-cyclopenta-[2,1-b:3,4-b′]dithiophene-*alt*-[2,1,3]-benzothiadiazole) (PCPDT-BT, Figure 2) and [6,6]-phenyl-C_{71}-butyric acid methyl ester ([70]PCBM). With an optical band gap of $E_g = 1.40$ eV in the film and an offset between the LUMOs corresponding to $\alpha \approx 0.55$ eV,[10] the maximum efficiency determined for PCPDT-BT:PCBM from Figure 1 is about $\eta = 6.2\%$. Figure 1 shows, however, that higher efficiencies can be expected for materials with slightly wider band gaps and that further gain may be expected when α becomes less to reduce the difference of ~0.75 eV between E_g (1.40 eV) and eV_{oc} (0.65 eV) for PCPDT-BT:PCBM.

Very recently a number of new alternating copolymers with CPDT have been reported. Moulé et al.[24] have described copolymers of CPDT alternating with with thiophene-benzothiadiazole-thiophene (PCPDT-TBTT) and with bis(ethylhexyl) quinoxaline (PCPDT-Q′) that both have higher band gaps ($E_g = 1.57$ eV) but unfortunately do not improve V_{oc} (0.60 and 0.64 V, respectively) when combined with [60]PCBM. You et al.[25] have synthesized polymers of CPDT alternating with benzodithiophene (BDT), naphthodithiophene (NDT), and dithienoquinoxaline (QDT) with optical band gaps in the range from 1.9–2.0 eV, but also here the V_{oc} (0.47–0.53 V) of cells with [60]PCBM decreased rather than increased compared to PCPDT-BT. Finally, Yang et al.[26] combined CPDT with benzoselenadiazole (BSe) to achieve a reduced band gap ($E_g = 1.35$ eV) polymer that gave $V_{oc} = 0.53$ V and $\eta = 0.89\%$ in combination with [70]PCBM. Each of these examples shows that substantial changes in materials properties can be achieved, but that improving V_{oc} with respect to E_g has not been achieved.

Here we present a series of alternating copolymers based on CPDT as an electron-rich unit and different electron-poor units (Figure 2) designed to control the band gap E_g ($=\alpha + \beta$) and the LUMO offset (α). The polymers, including PCPDT-BT, were synthesized via a palladium catalyzed Suzuki polymerization and have been analyzed for their optical, electrochemical, and photovoltaic properties. In the following we demonstrate that out of the series of CPDT-X polymers shown in Figure 2, two materials, PCPDT-BO and PCPDT-BBT, have more favorable energy levels and show promising photovoltaic response when mixed with [60]PCBM—equivalent or better than that of PCPDT-BT when prepared under similar conditions.

2. Results and Discussion

2.1. Synthesis

To obtain the alternating copolymers we employed a Suzuki polycondensation reaction using the bisboronic ester of CPDT that was synthesized as shown in Scheme 1. First, 3-bromothiophene (**1**) was lithiated and subsequently coupled with 3-thiophenecarboxaldehyde (**2**) to yield di-3-thienylmethanol (**3**). Without further purification **3** was reduced with $LiAlH_4$ to yield di-3-thienylmethane (**4**), which could be isolated more easily than **3**. The overall yield of the first two steps is about 88%. Direct bromination of **4** with *N*-bromosuccinimide (NBS) proceeded selectively at the 2 and 2′ positions to yield the dibrominated dithienomethane **5**. The subsequent intramolecular Ullmann coupling to 4*H*-cyclopenta[2,1-b:3,4-b′]dithiophene (CPDT, **6**) proceeded with microwave irradiation within 3 h at moderate yield (~30%). Recrystallization from methanol gave **6** as off-white flakes. Alkylation of **6** was achieved in the presence of a base and 2-ethylhexylbromide to give **7**. Bromination of **7** with NBS in *N*,*N*-dimethylformamide (DMF) gave **8**. Finally, monomer **9** was obtained by reacting **8** with BuLi and 2-isopropoxy-(1,3,2)-dioxaboralane in dry conditions. Bisboronic ester **9** was subjected to preparative recycling gas permeation

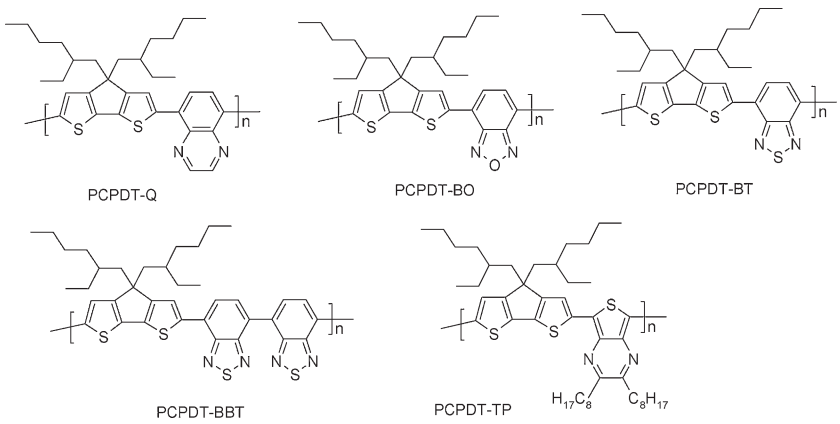

Figure 2. Alternating copolymers of CPDT with Q, BO, BT, BBT, and TP.

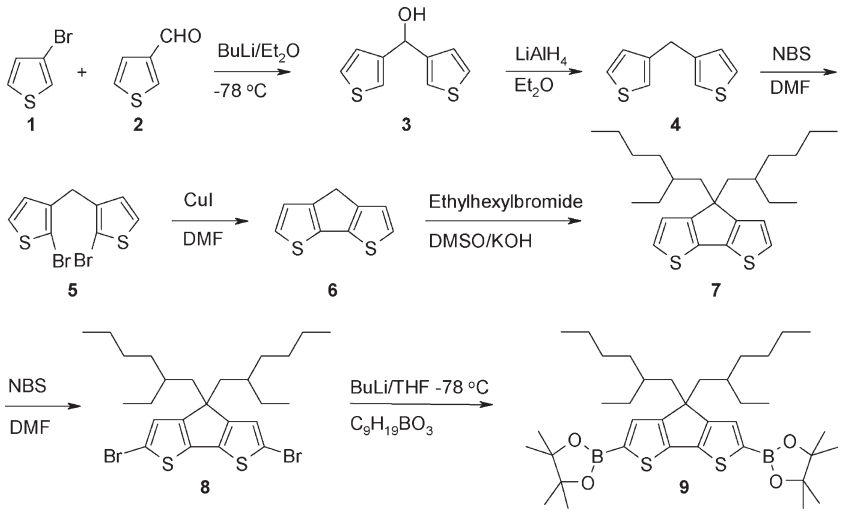

Scheme 1. Synthesis of CPDT co-monomer **9**.

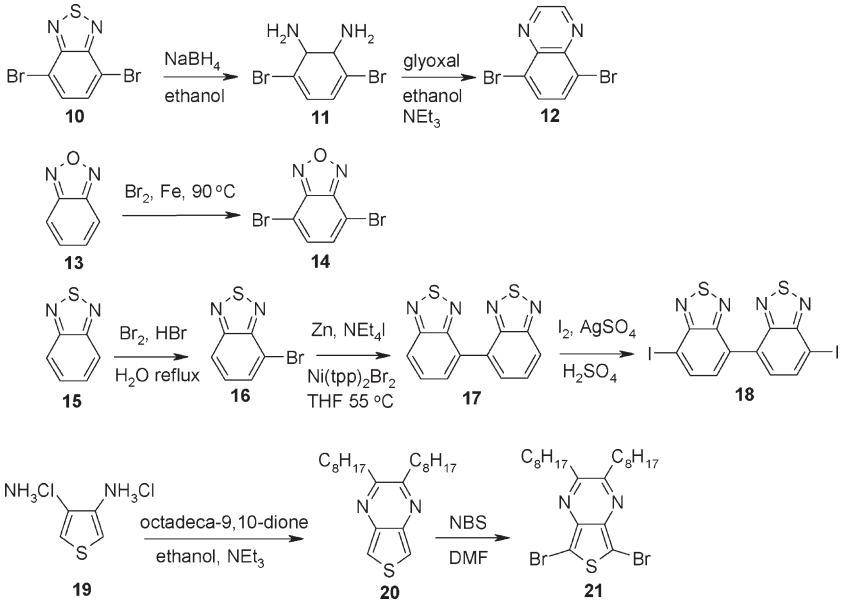

Scheme 2. Synthesis of electron-deficient co-monomers **12**, **14**, **18**, and **21**.

chromatography (GPC) in chloroform to remove traces of the corresponding monoboronic ester and enable high molecular weights in the Suzuki polymerization reactions.

The electron-poor moieties to be copolymerized with **9** were synthesized according to Scheme 2. Reduction of dibromobenzothiadiazole (**10**) with $LiAlH_4$ yielded diamine **11**, which was used without purification in a condensation reaction with aqueous glyoxal solution to yield monomer **12** as white needles. Bromination of benzooxadiazole (**13**) was done according to a literature procedure without solvent in a melt of **13**,[13] catalyzed by iron powder to yield monomer **14** as yellow crystals after recrystallization. Monobromination of benzothiadiazole (**15**) had only moderate yields (~30%). The monobrominated product **16** was used in a copper and zinc mediated Negishi type coupling to yield dibenzothiadiazole (**17**). Subsequent iodination with iodine in the presence of $AgSO_4$ yielded a yellow powder that was recrystallized from toluene to give monomer **18**. This compound was only sparingly soluble in common organic solvents such as chloroform and tetrahydrofuran (THF). The commercially available diamine **19** was directly converted via a condensation coupling to thienopyrazine **20**. The product was brominated with NBS to yield monomer **21** as a yellow solid, which had a limited stability.

All the dihalogenated monomers **10**, **12**, **14**, **18**, and **21** were copolymerized with **9** in a Suzuki type polycondensation to yield the copolymers depicted in Figure 2. The polymerizations were carried out for three days in degassed toluene with K_2CO_3 as the base. As a consequence, water and a phase transfer catalyst, Aliquat 336, were needed. After workup, fractionation with hexane and chloroform yielded the polymers PCPDT-Q, PCPDT-BO, PCPDT-BT, and PCPDT-BBT as dark-blue powders. PCPDT-TP was obtained as a dark-green powder. The typical yield of the polymerizations was in the range of 30%–70%. The molecular structure of the polymers was verified by ^{1}H-NMR spectroscopy.

2.2. Molecular Weights

The molecular weights of the polymers were determined with GPC at 80 °C in *o*-dichlorobenzene (*o*-DCB) relative to polystyrene standards, except for PCPDT-TP, which adsorbed to the column material in *o*-DCB and was therefore measured in THF at room temperature. The molecular weights (M_n) of the polymers range from 4 300 to 21 000 g mol^{-1} (Table 1), with polydispersity (PD) indices in the range of 1.4, except PCPDT-BO, which had a broader molecular weight distribution (PD = 1.95). The molecular weight of PCPDT-BBT is substantially lower, the M_n being 4 300 g mol^{-1}, which is probably due to the limited solubility of the polymer in the reaction mixture. All the synthesized polymers were very soluble in chlorobenzene (>5 mg mL^{-1}).

Table 1. Number and weight average molecular weights of PCPDT-X.

	M_n [g mol^{-1}]	M_w [g mol^{-1}]	PDI
PCPDT-Q	10 400	15 000	1.44
PCPDT-BO	21 000	41 000	1.95
PCPDT-BT	15 000	22 000	1.47
PCPDT-BBT	4 300	5 900	1.37
PCPDT-TP	8 900	12 200	1.38

2.3. Optical Properties

The normalized optical absorption spectra of the CPDT-X polymers in *o*-DCB solution and as thin films on glass (Figure 3)

Table 2. Optical gaps and redox potentials of PCPDT-X.

	E_g^{sol} [eV]	E_{ox}^{sol} [V] [a]	E_{red}^{sol} [V] [a]	E_{cv}^{sol} [eV]	ΔE^{sol} [eV]	E_g^{film} [eV]	α [eV]	β [eV]
PCPDT-Q	1.66	−0.06	−1.80	1.74	0.08	1.54	0.73	1.01
PCPDT-BO	1.54	+0.16	−1.52	1.68	0.14	1.47	0.45	1.23
PCPDT-BT	1.55	−0.07	−1.67	1.60	0.05	1.43	0.60	1.00
PCPDT-BBT	1.69	+0.22	−1.60	1.82	0.13	1.53	0.53	1.29
PCPDT-TP	1.24	−0.39	−1.73	1.34	0.10	1.18	0.66	0.68
PCBM			−1.07					

[a] Electrochemical potentials are versus Fc/Fc^+.

clearly show that these materials exhibit a strong absorption band in the long wavelength region extending beyond 1 000 nm for PCPDT-TP. The optical gaps (E_g) in solution and film have been determined from the crossing of the tangent in the inflection point with wavelength axis (Table 2). In thin films all polymers except PCPDT-TP exhibit optical gaps close to the ideal value of 1.5 eV (c.f. Figure 1) with gaps of Q and BBT being slightly larger than with BO and BT. The fact that the optical gap of PCPDT-BBT with the bis-BT moiety between the CPDT units is higher than that of PCPDT-BT, which has a single BT, is tentatively attributed to unfavorable steric interactions between the neighboring BT units in BBT that lead to twisting around their interring bonds, causing reduced conjugation. The thienopyrazine extends the absorption of PCPDT-BT well beyond 1 μm and creates an optical gap that is much smaller than any of the other polymers.[27,28]

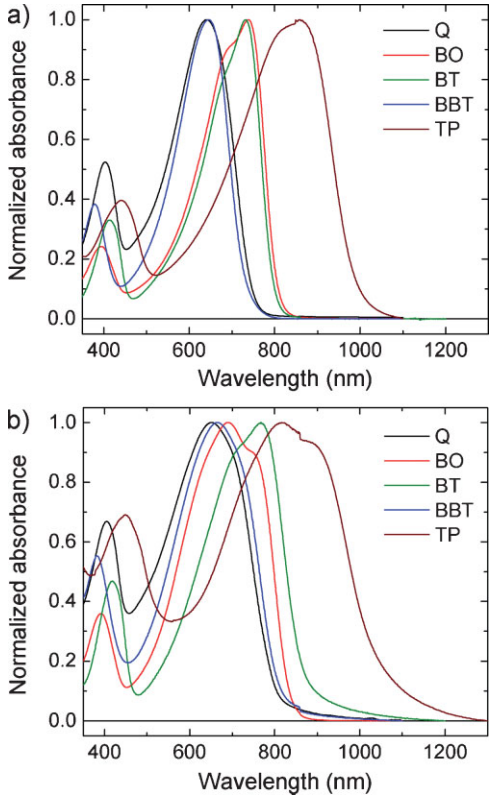

Figure 3. Normalized optical absorption spectra of PCPDT-X in o-DCB solution (a) and as thin film on glass (b).

2.4. Redox Properties

The electrochemical properties of the polymers were determined with cyclic voltammetry in *o*-DCB using tetrabutylammonium hexafluorophosphate ($TBAPF_6$) as an electrolyte. The onsets of the electrochemical reduction (E_{red}^{sol}) and oxidation (E_{ox}^{sol}) waves of the CPDT-X polymers are listed in Table 2 and shown in Figure 4. There is quite some spread between the oxidation potentials among the five polymers. PCPDT-TP is most readily oxidized. The oxidation potentials of PCPDT-BO and PCPDT-BBT are found at more positive values than for PCPDT-BT or PCPDT-Q, which is beneficial for reaching a higher open-circuit voltage in photovoltaic devices (vide infra). The reduction potentials vary less. For PCPDT-BBT the reduction potential is only slightly less than for PCPDT-BT, showing that the neighboring electron-deficient units do lead to better accepting properties but that the effect is small because of the steric hindrance between the two BT units (vide supra).

For a copolymer with alternating electron-rich (CPDT) and electron-deficient units (X), one might expect that by changing X, only the LUMO would be affected. However, Figure 4 clearly shows that the X unit in PCPDT-X can have an equally large effect on the HOMO (E_{ox}^{sol}) level of the polymer as on the LUMO (E_{red}^{sol}) level. For X = TP the effect on the HOMO level is even much more pronounced. Apparently, TP is both a better donor and a better acceptor than CPDT. In our view, the reduction of the band gap of PCPDT-TP is primarily caused by introducing TP units and less by the alternation of CPDT and TP. This is in accordance with the fact that the band gap of polythienopyrazine (poly-TP)[28,29] is lower than that of PCPDT-TP. Similar

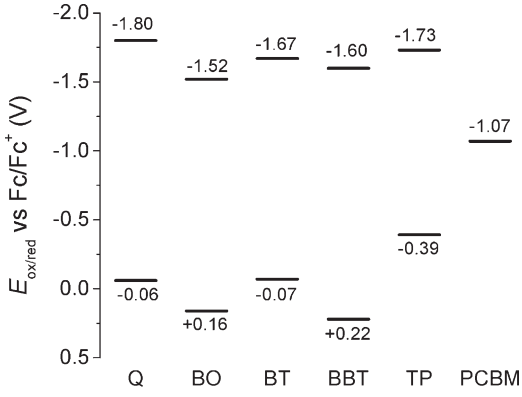

Figure 4. Electrochemical potentials of PCPDT-X and [60]PCBM.

arguments, although less evident, will apply to the other PCPDT-X polymers. This shows that naming these materials alternating electron-rich and -deficient copolymers is maybe less appropriate.

The electrochemical gap defined as $E_{cv}^{sol} = e(E_{red}^{sol} - E_{ox}^{sol})$ (with e the charge of the electron) follows the same trend as the optical gap (E_g^{sol}) measured in the same solvent but is consistently somewhat larger by $\Delta E^{sol} = 0.08$–0.14 eV. Such a small difference is not unexpected because for determining E_{ox} and E_{red} electrons are extracted or added, whereas the optical gap provides the energetic difference for an intramolecular excitonic state, with the hole and the electron stabilized by Coulomb attraction.

Taking the onsets of the oxidation and reduction potentials as a measure for the HOMO and LUMO levels, it is possible to estimate the α and β values for these polymers as defined in Figure 1 (see Table 2) by comparing with the reduction of [60]PCBM (-1.07 V vs. Fc/Fc^+). The resulting values for $\alpha = e(E_{red} - 1.07)$ and $\beta = e(-1.07 - E_{ox})$ are collected in Table 2 and reveal that for each CPDT-X polymer photoinduced electron transfer can be expected ($\alpha > 0.4$ eV) and that the open-circuit voltage should increase from X = TP via Q, BT, and BO, to BBT. More interestingly, using α and β and the optical gap in the film and the assumptions outlined in the introduction, we can make some prediction with respect to maximum attainable efficiencies using the diagram of Figure 1. The resulting values 4.7% (Q), 7.9% (BO), 5.7% (BT), 7.0% (BBT), <2.2% (TP) indicate that PCPDT-BO and PCPDT-BBT are promising materials for photovoltaics considering their frontier orbital energies.

2.5. Photovoltaic Devices

Solar cells were fabricated on glass substrates with a transparent indium tin oxide (ITO)/poly(3,4-ethylenedioxythiophene):poly-(styrene sulfonate) (PEDOT: PSS) front electrode and a reflecting LiF/Al back electrode. The active layers were spin coated from chlorobenzene solutions of the polymer and [60]PCBM. The weight ratio PCPDT-X:[60]PCBM in the solution was 1:3 and for each polymer the layer thickness was optimized for optimal performance by varying the spin speed. The current density verses voltage (J–V) curves, measured under simulated solar light (100 mW cm^{-2}), are depicted in Figure 5a. The monochromatic EQE (Figure 5b) was measured under bias light corresponding to approximately 1 sun intensity. The relevant parameters are summarized in Table 3 together with an overview of literature

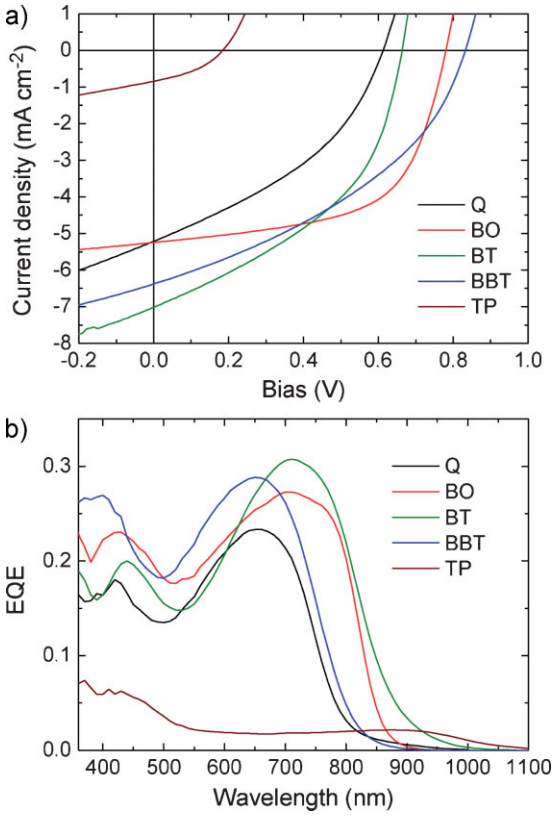

Figure 5. a) J–V curves of the photovoltaic devices made or PCPDT-X:[60]PCBM (1:3). b) Spectrally resolved EQE measured with 532 nm bias illumination with an intensity set to give J_{sc} corresponding to ~1 sun intensity.

Table 3. Characteristics of PCPDT-X:PCBM photovoltaic cells.

	V_{oc} [V]	J_{sc} [mA cm^{-2}]	J_{sc}(SR) [c] [mA cm^{-2}]	FF	η [%]	d [nm]	Reference
PCPDT-Q	0.61	5.2	4.6	0.39	1.1 [d]	79	This work
PCPDT-BO	0.78	5.2	5.4	0.60	2.5 [d]	94	This work
PCPDT-BT	0.66	7.0	6.5	0.44	1.9 [d]	98	This work
PCPDT-BT	0.65	9.0	–	0.45	2.7	150–250	[10]
PCPDT-BT [a]	0.65	11.0	–	0.47	3.2	150–250	[10]
PCPDT-BT [a,b]	0.62	16.2	–	0.55	5.5	110	[2]
PCPDT-BBT	0.83	6.4	6.1	0.39	2.0 [d]	71	This work
PCPDT-TP	0.18	0.9	1.0	0.38	0.1 [d]	74	This work
PCPDT-TBTT	0.60	8.3	–	0.42	2.1	70	[24]
PCPDT-Q′	0.64	2.4	–	0.48	0.7	70	[24]
PCPDT-BDT	0.47	2.5	–	0.32	0.4	90	[25]
PCPDT-NDT	0.47	3.6	–	0.33	0.6	90	[25]
PCPDT-QDT	0.53	4.6	–	0.47	1.1	100	[25]
PCPDT-BSe [a]	0.52	5.0	–	0.34	0.9	60	[26]

[a] Using [70]PCBM. [b] Using octanedithiol as a processing agent during film formation. [c] Using convolution of the spectral response with the AM1.5G emission. [d] Based on Jsc(SR).

data on related CPDT based polymers. We note that the difference in molecular weights of the polymers hampers a direct comparison of the device parameters, especially because short-circuit current and fill factor are often negatively affected by too low molecular weights.[30,31] For PCPDT-BT the molecular weight has been found critical for attaining the desired morphology and efficiency.[32,33]

For PCPDT-BT:[60]PCBM we obtain a very similar performance to that found by Mühlbacher et al.,[10] with nearly identical V_{oc}, FF, and an EQE that maximizes at 31%. Our estimate of the short circuit current of $J_{sc}(SR) = 6.5\ mA\ cm^{-2}$ is, however, slightly lower than the $9\ mA\ cm^{-2}$ previously reported, which results in a lower estimated efficiency of $\eta = 1.9\%$ compared to $\eta = 2.67\%$.[10] The difference is most likely due to differences in the white-light spectra used in the two studies.

Each of the other four polymers also shows a significant photovoltaic effect. As expected from the oxidation potentials, the V_{oc} for cells with PCPDT-BO and PCPDT-BBT is higher than that of PCPDT-BT. For both polymers the energy loss from E_g to eV_{oc} is 0.7 eV, which places these two polymers closer to the energy conversion optimum in Figure 1 than PCPDT-BT. In fact, the 0.7 eV difference approaches the 0.6 eV that was recently predicted as being the minimum loss in bulk heterojunction solar cells.[34] The maximum EQE values for the two polymers (27% and 29% for BO and BBT, respectively) are slightly lower than that of PCPDT-BT. The good FF and the increased V_{oc} of the PCPDT-BO:[60]PCBM cell makes its power conversion efficiency superior to that of the others polymers. The performance of PCPDT-Q is significantly less than that of PCPDT-BT, mainly due to a loss in short-circuit current. Finally, PCPDT-TP shows the most red-shifted response of all polymers, beyond 1 μm (Figure 5b), but since the EQE remains small the photocurrent is low. The high HOMO level of PCPDT-TP causes a loss of V_{oc} and with $\eta = 0.1\%$, the overall performance is low.

Comparing eV_{oc} for the five polymers with the β values in Table 2 reveals a similar trend with an offset of 0.42 ± 0.08 eV. This demonstrates that the oxidation potential of the donor and the reduction potential of the acceptor as determined in solution can be used to obtain a fairly accurate estimate of V_{oc}. The offset of 0.42 ± 0.08 V is close to the value of 0.4 eV predicted by Blom et al.[18] and the value of 0.43 eV found by Manca et al.[35] for the difference between eV_{oc} and the absorption band to charge transfer state.

The fill factor for the solar cells are in the range FF = 0.38–0.44 for these polymers, except for PCPDT-BO where FF = 0.60. A low fill factor is often associated with strongly unbalanced charge transport that leads to space-charge-limited photocurrents. However, for PCPDT-BT:[60]PCBM, the origin of the low fill factor has recently been studied in more detail by Blom et al.[36] They showed that the low FF (=0.40 in Reference [36]) was due to the short lifetime of the bound electron–hole pairs at the donor/acceptor interface. Although we cannot speculate on the reasons for the low FF for the other three polymers, it is clear that for PCPDT-BO, that gives FF = 0.60, neither charge transport nor electron–hole pair lifetime seem to limit the performance.

From Table 3, PCPDT-BT, PCPDT-BBT, and PCPDT-BO clearly identify as providing the best efficiencies. Detailed studies for PCPDT-BT have revealed that a high molecular weight for obtaining a high hole mobility[37] and the addition of processing agents[38] are key parameters for further improving the efficiency of these solar cells, in addition to the use of [70] PCBM to enhance the absorption in the visible spectral region. Our study reveals that PCPDT-BBT and PCPDT-BO are interesting leads for such further optimization of molecular weight and processing conditions. Their initial performance is good and their energy levels are positioned more favorable than that of PCPDT-BT with respect to PCBM.

3. Conclusions

Alternating copolymers using an electron-rich CPDT unit and five different electron-deficient aromatic units (Figure 2) have been synthesized via a Suzuki polymerization reaction. The optical absorption and electrochemical potentials were used to determine the relevant energy levels of these CPDT-X polymers The photovoltaic devices of the corresponding PCPDT-X:[60]PCBM donor:acceptor blends revealed that the open-circuit voltages of the cells correspond to the expected values based on the redox potentials. The best solar cells were made with polymers based on CPDT with BO or BBT as electron-deficient unit. Mixed with PCBM these polymers showed an open-circuit voltage that is significantly higher than that of PCPDT-BT. The best device was based on a PCPDT-BO:PCBM blend and gave $J_{sc} = 5.4\ mA\ cm^{-2}$, FF = 0.6, and $V_{oc} = 0.78$ V, resulting in a maximum power conversion efficiency of over 2.5% at an optical band gap of $E_g = 1.47$ eV. The energy loss from E_g to eV_{oc} is 0.69 V and one of the lowest values reported for bulk-heterojunction solar cells, close to the expected minimum loss of 0.6 V.[34]

4. Experimental

All synthetic procedures were performed under an argon atmosphere. Commercial chemicals were used as received. Dry solvents were distilled over 4 Å molecular sieves. ^{1}H-NMR and ^{13}C-NMR spectra were recorded at 400 and 100 MHz, respectively, on a VARIAN mercury spectrometer with $CDCl_3$ as the solvent and tetramethylsilane (TMS) as the internal standard. The peaks are given in ppm relative to TMS (0 ppm). Molecular weights were determined with GPC at 80 °C on a PL-GPC 120 system using a PL-GEL 5 μ MIXED-C column and *o*-DCB as the eluent. For PCPDT-TP a PLgel MIXED-C in series with a PLgel MIXED-D column at room temperature was used with THF as the eluent. UV–Vis spectra were recorded on a Perkin Elmer Lambda 900 Uv–Vis–nearIR spectrophotometer. Cyclic voltammograms were recorded with a scan rate of $0.1\ V\ s^{-1}$ under an inert atmosphere with 1 M $TBAPF_6$ in *o*-DCB as the electrolyte. The working electrode was a platinum disk and the counter electrode was a platinum electrode. The concentration of the samples in the electrolyte was approximately 2 M, based on monomers. Fc/Fc^+ was used as internal standard. Recycling GPC was performed with a JAIGEL 2H and a 2.5H column attached to a LC system equipped with a UV detector with a path of 0.5 mm and a switch for recycling and collecting the eluent. The eluent was chloroform at $3.5\ mL\ min^{-1}$ and the injection volume was 1 mL. Photovoltaic devices were processed on cleaned patterned ITO glass substrates. A mixed solution of polymer and [60]PCBM (Solenne BV) in a 1:3 weight ratio was spin coated from chlorobenzene on 50 nm of PEDOT:PSS (Clevios P VP AI 4083, H.C. Starck). The devices were transported into a glovebox with nitrogen atmosphere. LiF (1 nm) and aluminum (100 nm) were thermally evaporated on top of the active layer at a pressure of 10^{-7} mbar. The devices had an active area of $0.091\ cm^2$, which is determined by the overlap of the ITO and the evaporated aluminum. Current–voltage curves were measured with a Keithley 2400 source meter under illumination of simulated solar light in nitrogen atmosphere. Spectral response curves were measured with a Stanford Research Systems

Model SR830 DSP lock-in-amplifier by using modulated monochromatic light from a tungsten halogen lamp in combination with a monochromator (Oriel, Cornerstone 130). During the measurement the device was operating at 1 equivalent sun intensity by use of a bias laser (532 nm). A calibrated Si cell was used as a reference. The device was kept behind a quartz window in a nitrogen-filled container. The thickness of the active layers in the photovoltaic devices was measured on a Veeco Dektak150 profilometer.

*Di-3-thienylmethanol (**3**)*: n-BuLi in hexanes (15.7 mL, 2.5 M) was slowly added to a solution of **1** (3.3 mL, 5.7 g, 3.5 mmol) in dry diethyl ether (100 mL) at −75 °C. The mixture was stirred for 30 min at −78 °C. Then **2** (3.13 mL, 4.0 g, 3.6 mmol) was added dropwise. This mixture was allowed to reach room temperature overnight. The reaction mixture was washed with acid, base, and brine. The organic layer was dried on sodium sulfate and the solvent was evaporated under reduced pressure. The crude product, which was 90% pure, was taken to the next reaction without further purification.

*Di-3-thienylmethane (**4**)*: $AlCl_3$ (4.70 g, 35 mmol) was added to a solution of $LiAlH_4$ (1.32 g, 35 mmol) in dry diethyl ether (100 mL) at room temperature. To this mixture crude **3** (6.68 g) was added dropwise. This mixture was refluxed for 3 h after which the reaction mixture was washed with hydrochloric acid (150 mL, ∼1 M), NaOH solution (150 mL, ∼1 M), and twice with brine (150 mL). All water layers were once extracted with diethyl ether. The combined organic layers were dried on sodium sulfate and subjected to column chromatography (silica, heptane). This resulted in 4.56 g (25 mmol, 88%) of **4** as a colorless oil. ^{1}H-NMR: 7.26 (dd, J = 3.6 Hz, 2H), 6.95 (dd, J = 4.2Hz, 2H), 6.94 (t, J = 4.8 Hz, 2H), 3.99 (s, 2H). ^{13}C-NMR: 140.99 (q), 128.40 (t), 125.61 (t), 121.17 (t), 31.11 (s).

*Bis(2-bromothien-3-yl)methane (**5**)*: NBS (9.01 g, 51 mmol) was slowly added to an ice-cooled and stirred solution of **4** (4.56 g, 25 mmol) in DMF (200 mL). The mixture was allowed to reach room temperature overnight and then extracted with diluted hydrochloric acid and diethyl ether. The diethyl ether layer was washed with water and brine. The organic solvent layers were evaporated under reduced pressure and column chromatography (silica, eluent heptane) yielded **5** (7.31 g, 21.6 mmol, 86%) of a colorless oil. ^{1}H-NMR: 7.18 (d, J = 5.2 Hz, 2H), 6.73 (d, J = 6.0 Hz, 2H), 3.86 (s, 2H). ^{13}C-NMR: 138.79 (q), 128.46 (t), 125.70 (t), 109.80 (q), 29.47 (s).

*4H-Cyclopenta[2,1-b:3,4-b′]dithiophene (**6**)*: **5** (3.01 g 8.9 mmol) was added to activated copper bronze (6.1 g, 96 mmol) in dry DMF (200 mL). This mixture was stirred in a Milestone MicroSYNTH microwave reactor at 140 W at an internal temperature of 145 °C for 3 h. The reaction mixture was repeatedly extracted with water and heptane and the organic layers were combined. The solids that resulted after evaporation of the organic solvent were recrystallized from methanol to yield **6** (0.73 g, 4.1 mmol, 47%) as off-white flakes. ^{1}H-NMR: 7.18 (d, J = 5.2 Hz, 2H), 7.09 (d, J = 4.8 Hz, 2H), 3.54 (s, 2H). ^{13}C-NMR: 149.65 (q), 138.64 (q), 124.45 (t), 122.94 (t), 31.81 (s).

*4,4-Di(2-ethtylhexyl)-4H-cyclopenta[2,1-b:3,4-b′]dithiophene (**7**)*: To a solution of **6** (4.23 g, 24 mmol) in DMSO, powdered KOH (4.80 g, 86 mmol), and KI (30 mg, 0.2 mmol) were added, followed by 2-ethylhexylbromide (10.67 g, 55 mmol). This mixture was stirred at room temperature overnight and then poured out in water and heptane. The organic layer was washed two times with water and one time with brine. The heptane was evaporated in vacuo and the resulting light yellow oil was subjected to column chromatography (silica, eluent heptane) to yield **7** as a light-yellow oil (8.49 g, 21 mmol, 89%). ^{1}H-NMR: 7.10 (d, J = 4.4 Hz, 2H), 6.91 (m, 2H), 1.85 (m, 2H), 0.90 (m, 18H), 0.75 (t, 2H), 0.58 (t, 2H). ^{13}C-NMR: 157.59 (q), 136.77 (q), 123.92 (t), 122.30 (t), 53.22 (q), 43.21 (s), 34.97 (s), 34.11 (s), 28.57 (s), 27.24 (s), 22.74 (s), 14.07 (p), 10.63 (p).

*2,6-Dibromo-4,4-di(2-ethylhexyl)-4H-cyclopenta[2,1-b:3,4-b′]dithiophene (**8**)*: NBS (380 mg, 2.13 mmol) was added in small portions to a solution of **7** (390 mg, 0.97 mmol) in DMF (25 mL). This mixture was stirred overnight, after which of water (50 mL) was added and the water layer was extracted with diethyl ether. The organic layer was dried on $MgSO_4$ and the solvents from the organic layer were evaporated. The resulting yellow oil was subjected to column chromatography (silica, eluent heptane) to yield **8** (480 mg, 0.86 mmol, 88%) as a light-yellow oil. ^{1}H-NMR: 6.93 (t, J = 3.2 Hz, 2H), 1.80 (m, 4H), 1.26 (m, 2H), 0.9 (m, 16H), 0.78 (m, 6H), 0.62 (m, 6H). ^{13}C-NMR: 155.56 (q), 136.60 (q), 125.21 (q), 110.68 (q), 54.95 (q), 43.03 (s), 35.09 (s), 34.02 (t), 28.53 (s), 27.28 (s), 22.76 (s), 14.06 (p), 10.64 (p).

*2,6-Bis(4,4,5,5-tetramethyl-1,3,2-dioxaboralan-2-yl)-4,4-di(2-ethylhexyl)-4H-cyclopenta-[2,1-b:3,4-b′]dithiophene (**9**)*: A n-BuLi solution in hexanes (1.1 mL, 2.5 M) was added at −70 °C to a solution of **8** (260 mg, 0.46 mmol) in dry THF (20 mL). The mixture was stirred for 30 min at −70 °C, after which 2-isopropoxy-(1,3,2)-dioxaboralane (0.5 mL, 0.46 g, 2.4 mmol) was added at −70 °C. This mixture was allowed to reach room temperature overnight. The reaction mixture was poured out in water and diisopropyl ether, and the organic layer was washed with brine. The solvents were evaporated from the organic layer and the resulting oil was subjected to column chromatography (eluent heptane/ethyl acetate 97:3). This yielded a light-green oil that was then subjected to recycling GPC in $CHCl_3$. This resulted in **9** (185 mg, 0.28 mmol, 61%) as a slightly yellow sticky oil. ^{1}H-NMR: 7.44 (t, 2H), 1.83 (m, 4H), 1.3 (s, 24H), 0.9(m, 18H), 0.73 (m, 6H), 0.58 (m, 6H). ^{13}C-NMR: 160.99 (q), 144.10 (q), 131.90 (q), 83.94 (t), 52.68 (q), 43.21 (s), 35.14 (s), 33.85 (s), 29.72 (q), 28.33 (s), 27.43 (s), 24.75 (p), 22.79(s), 14.10 (p), 10.59 (p).

*5,8-Dibromoquinoxaline (**12**)*: $NaBH_4$ (2.18 g, 58 mmol) was added in small portions to **10** (1.0 g, 3.40 mmol) dissolved in ethanol (25 mL) at room temperature. This mixture was stirred overnight, after which diethyl ether and water were added. The organic layer was washed three times with water and one time with brine. The solvents from the organic layer were evaporated and the resulting white solid **11** was used without further purification. To a solution of **11** in ethanol (30 mL), 40 wt% glyoxal in water (1.5 mL) was added, followed by 2 drops of dry triethylamine. This mixture was stirred at room temperature overnight. The white crystals that had formed were filtered off and recrystallized from ethanol to give **12** as white needles (760 mg, 2.64 mmol, 76%). ^{1}H-NMR: 9.01 (s, 2H), 8.00 (s, 2H). ^{3}C-NMR: 146.04 (t), 141.57 (q), 133.72 (t), 123.98 (q).

*4,7-Dibromobenzoxadiazole (**14**)*: Bromine (15.2 g, 95 mmol) was added dropwise to a melt of **13** (4.86 g, 40.4 mmol) at 90 °C containing iron dust (93 mg, 1.6 mmol). After stirring 2 h at 90 °C the mixture was poured out in water. A solution of sodium bisulfite was added until no gas evolution was observed. The solid was filtered off and impregnated on silica. This was subjected to column chromatography (silica, eluent heptane). The resulting yellow solid was recrystallized in ethanol to yield **14** (8.40 g, 30 mmol, 75%) as yellow crystals. ^{1}H-NMR: 7.51 (s, 2H). ^{13}C-NMR: 149.38 (q), 134.17 (q), 108.70 (q).

*4-Bromo-2,1,3-benzothiadiazole (**16**)*: **15** (14.3 g. 105 mmol) was dissolved in aqueous 48 wt% HBr (125 mL) at 150 °C and bromine (5.9 mL, 18 g, 115 mmol) was added slowly. This mixture was stirred for 2 h at 150 °C, after which GC-MS analysis showed that there was about 40% nonbrominated product. Then an additional amount of bromine (6 g, 38 mmol) was added. The resulting mixture was refluxed for another 3 h. The reaction mixture was cooled down to room temperature poured out in of ice water (800 mL), after which saturated $Na_2S_2O_5$ solution was added until the water was colorless. The water layer was extracted with diethyl ether. The solvent of the organic layer was evaporated and the solid was subjected to column chromatography (silica, eluent ethyl acetate and heptane) to yield **16** (7.41 g, 34 mmol, 32%) as a white solid. ^{1}H-NMR: 7.97 (d, J = 8.8 Hz, 1H), 7.84 (d, J = 8.8 Hz, 1H), 7.48 (t, J = 8.8 Hz, 1H). ^{13}C-NMR: 154.61 (q), 153.37 (q), 131.99 (t), 129.93 (t), 120.90 (t), 114.43 (q).

*4,4′-Bis(2,1,3-benzothiadiazole) (**17**)*: To a solution of tetraethylammonium iodide (2.93 g, 1.14 mmol), zinc powder (1.14 g, 17 mmol), and di(triphenylphosphine)nickel dibromide (2.46 g, 3.36 mmol) in THF (20 mL), a solution of **16** (2.50 g, 11.6 mmol) was added slowly. The resulting mixture was heated to 55 °C for 8 h, after which it was poured out in $CHCl_3$ (50 mL). The solvents were evaporated and the crude product was impregnated on silica and subjected to column chromatography (silica, dichloromethane). The resulting white product was recrystallized from ethanol to yield **17** (804 mg, 2.97 mmol, 51%) as a yellow powder. ^{1}H-NMR: 8.27 (d, J = 6.8 Hz, 2H), 8.12 (d, J = 8.8 Hz, 2H), 7.81 (t, J = 7.2 Hz, 2H). ^{13}C-NMR: 155.47 (q), 153.59 (q), 130.77 (t), 129.99 (q), 129.44 (t), 121.64 (t).

*7,7′-Diiodo-4,4′-bis(2,1,3-benzothiadiazole) (**18**)*: $AgSO_4$ (1.06 g, 3.40 mmol) in sulfuric acid (2.5 mL) was stirred until the solid was dissolved. Iodine (278 mg, 1.10 mmol) was added and the solution was stirred for 3 h at room temperature until all the iodine had dissolved. The mixture was then added to **17** (100 mg, 0.37 mmol) at 110 °C. The resulting mixture was stirred at 110 °C for 1 h, after which it was poured out in water (100 mL). The yellow water layer was extracted repeatedly with chloroform until the extracts were colorless. The solvents were evaporated from the organic layer and the yellow substance was recrystallized from toluene to yield **18** (132 mg, 0.25 mmol, 69%) as a yellow powder. ^{1}H-NMR: 8.30 (d, $J = 8.0$ Hz, 2H), 8.06 (d, $J = 8.0$ Hz, 2H). The product was not soluble enough to perform ^{13}C NMR spectroscopy.

*2,3-Di-n-octylthieno[3,4-b]pyrazine (**20**)*: To a solution of 3,4-diaminothiophene dihydrochloride (***19***) (325 mg, 1.72 mmol) and octadeca-9,10-dione (800 mg, 2.84 mmol) in ethanol (20 mL), triethylamine (1 mL) was added. The mixture was stirred for 2 h at room temperature, after which the solvents were evaporated and the solid extracted with heptane. The heptane was evaporated and the resulting whitish solid was subjected to column chromatography (silica, heptane, and ethyl acetate) to yield **20** (412 mg, 1.14 mmol, 67%) as a yellow solid. ^{1}H-NMR: 7.79 (s, 2H), 2.88 (t, $J = 8.0$ Hz, 4H), 1.78 (t, $J = 8.0$ Hz, 4H), 1.45 (m, 4H), 1.3 (m, 16H), 0.87 (t, $J = 6.8$ Hz, 6H). ^{13}C-NMR: 156.39 (q), 141.64 (q), 11.79 (t), 35.75 (s), 31.85 (s), 29.72 (s), 29.44 (s), 29.23(s), 28.39 (s), 22.67 (s), 14.10 (p).

*5,7-Dibromo-2,3-di-n-octylthieno[3,4-b]pyrazine (**21**)*: NBS (148 mg 0.91 mmol) in DMF (3 mL) was slowly added to a solution of 2,3-di-*n*-octylthieno[3,4-*b*]pyrazine (153 mg, 0.42 mmol) in DMF (10 mL) at −15 °C. This mixture was stirred in dark conditions at room temperature overnight. The reaction mixture was poured out in water (50 mL) and diethyl ether (50 mL). The water layer was extracted until the extracts were colorless. The solvents of the organic layers were evaporated without heat. The solid was subjected to column chromatography (silica, pentane and dichloromethane) to yield **21** (130 mg, 0.25 mmol, 60%) as a yellow solid. ^{1}H-NMR: 2.89 (t, $J = 8.0$ Hz, 4H), 1.80 (q, $J = 7.6$ Hz, 4H), 1.45 (m, 4H), 1.3 (m, 16H), 0.89 (t, $J = 6.4$ Hz, 6H). ^{13}C-NMR: 158.16 (q) 139.34 (q), 103.09 (q), 35.33 (s), 31.84 (s), 29.56 (s), 29.42 (s), 29.22 (s), 27.93 (s), 22.66 (s), 14.10 (p).

PCPDT-Q: To a degassed solution of **9** (65 mg, 0.10 mmol), **12** (28 mg, 0.10 mmol), 1 drop of Aliquat 336, and 2 M K_2CO_3 in degassed water (0.2 mL) in toluene (3 mL), tetrakis(triphenylphosphine)palladium(0) (2 mg, 1.7 μmol) was added. This mixture was stirred at 115 °C for three days, after which it was precipitated in methanol. The solids were filtered off, redissolved in $CHCl_3$ (75 mL) and refluxed with 28% NH_3 solution in water (75 mL) for 3 h. The layers were separated and the organic layer was stirred with ethylenediaminetetraacetic acid (250 mg) overnight, after which water (100 mL) was added and the liquids were stirred for 1 h. The layers were separated and the organic layer was reduced in volume by evaporating most of the chloroform. The polymer was precipitated in methanol and filtered through a soxhlet thimble. The polymer was extracted with methanol, after which the thimble was allowed to dry in ambient conditions. Then the polymer was extracted with hexane and chloroform. The solvent from the chloroform fraction was evaporated and the solid was precipitated in methanol. The polymer was collected by filtering over a 0.45 μm poly(tetrafluoroethylene) membrane filter and dried in a vacuum oven to yield PCPDT-Q (15 mg, 29%) as a dark-blue powder. ^{1}H-NMR: 9.00 (b, 2H), 8.15 (b, 2H), 7.80 (b, 2H), 2.05 (b, 4H), 1.00 (b, 18H), 0.65 (b, 12H).

PCPDT-BO: Identical procedure as for PCPDT-Q, using **9** and **14**, yield: 68% as a dark-blue powder. ^{1}H-NMR: 8.05 (b, 2H), 7.55 (b, 2H), 2.10 (b, 4H), 1.00 (b, 18H), 0.65 (b, 12H).

PCPDT-BT: Identical procedure as for PCPDT-Q, except at 80 °C using **9** and **10**, yield: 72% as a dark-blue powder. ^{1}H-NMR: 8.13 (b, 2H), 7.88 (b, 2H), 2.05 (b, 4H), 1.0 (b, 18H), 0.80 (b, 6H), 0.65 (b, 6H).

PCPDT-BBT: Identical procedure as for PCPDT-Q, using **9** and **18**, yield: 40% as a dark-blue powder. ^{1}H-NMR: 8.45 (b, 2H), 8.30 (b, 2H), 8.00 (b, 2H), 2.05 (b, 4H), 1.05 (b, 18H), 0.65 (b, 12H).

PCPDT-TP: Identical procedure as for PCPDT-Q, using **9** and **21**, yield: 32% as a dark-green powder. ^{1}H-NMR: 7.45 (b, 2H), 3.00 (b, 4H), 2.00 (b, 8H), 1.36, (b, 14H), 1.00 (b, 24H), 0.70 (b, 18H).

Acknowledgements

The research was supported by a TOP grant of the Chemical Sciences (CW) division of the Netherlands Organization for Scientific Research (NWO) and is part of the Joint Solar Programme (JSP). The JSP is cofinanced by the Foundation for Fundamental Research on Matter (FOM), Chemical Sciences of NWO, and the Foundation Shell Research. The work of M.S. is part of the research program of the Dutch Polymer Institute (DPI, project 524). The work of J.G. is supported by Senter/Novem in the EOS project Zomer (EOSLT03026).

Received: March 10, 2009
Revised: June 11, 2009
Published online: September 3, 2009

[1] B. C. Thompson, J. M. J. Fréchet, *Angew. Chem. Int. Ed.* **2008**, *47*, 58.
[2] J. Peet, J. Y. Kim, N. E. Coates, W. L. Ma, D. Moses, A. J. Heeger, G. C. Bazan, *Nat. Mater.* **2007**, *6*, 497.
[3] Y. Liang, Y. Wu, D. Feng, T.-S. Tsai, H.-J. Son, G. Li, L. Yu, *J. Am. Chem. Soc.* **2009**, *131*, 56.
[4] A. Dhanabalan, J. K. J. Van Duren, P. A. van Hal, J. L. J. van Dongen, R. A. J. Janssen, *Adv. Funct. Mater.* **2001**, *11*, 255.
[5] X. Wang, E. Perzon, J. L. Delgado, P. De la Cruz, F. Zhang, F. Langa, M. R. Andersson, O. Inganäs, *Appl. Phys. Lett.* **2004**, *85*, 5081.
[6] O. Inganäs, M. Svensson, F. Zhang, A. Gadisa, N. K. Persson, X. Wang, M. R. Andersson, *Appl. Phys. A* **2004**, *79*, 31.
[7] L. M. Campos, A. Tontcheva, S. Günes, G. Sonmez, H. Neugebauer, N. S. Sariciftci, F. Wudl, *Chem. Mater.* **2005**, *17*, 4031.
[8] F. Zhang, W. Mammo, L. M. Andersson, S. Admassie, M. R. Andersson, O. Inganäs, *Adv. Mater.* **2006**, *18*, 2169.
[9] Y. J. Xia, X. Y. Deng, L. Wang, X. Z. Li, X. H. Zhu, Y. Cao, *Macromol. Rapid Commun.* **2006**, *27*, 1260.
[10] D. Mühlbacher, M. Scharber, M. Morana, Z. Zhu, D. Waller, R. Gaudiana, C. Brabec, *Adv. Mater.* **2006**, *18*, 2884.
[11] M. M. Wienk, M. Turbiez, J. Gilot, R. A. J. Janssen, *Adv. Mater.* **2008**, *20*, 2556.
[12] J. Hou, H.-Y. Chen, S. Zhang, G. Li, Y. Yang, *J. Am. Chem. Soc.* **2008**, *130*, 16144.
[13] N. Blouin, A. Michaud, G. Gendron, S. Wakim, E. Blair, R. Neagu-Plesu, M. Belletete, G. Durocher, Y. Tao, M. Leclerc, *J. Am. Chem. Soc.* **2008**, *130*, 732.
[14] E. Zhou, M. Nakamura, T. Nishizawa, Y. Zhang, Q. Wei, K. Tajima, C. Yang, K. Hashimoto, *Macromolecules* **2008**, *41*, 8302.
[15] C. Kitamura, S. Tanaka, Y. Yamashita, *Chem. Mater.* **1996**, *8*, 570.
[16] M. C. Scharber, D. Mühlbacher, M. Koppe, P. Denk, C. Waldauf, A. J. Heeger, C. J. Brabec, *Adv. Mater.* **2006**, *18*, 789.
[17] C. J. Brabec, A. Cravino, D. Meissner, N. S. Sariciftci, T. Fromherz, M. T. Rispens, L. Sanchez, J. C. Hummelen, *Adv. Funct. Mater.* **2001**, *11*, 374.
[18] V. D. Mihailetchi, P. W. M. Blom, J. C. Hummelen, M. T. Rispens, *J. Appl. Phys.* **2003**, *94*, 6849.
[19] A. Gadisa, M. Svensson, M. R. Andersson, O. Inganäs, *Appl. Phys. Lett.* **2004**, *84*, 1609.
[20] We note that any other value assumed for FF or EQE would simply cause a proportional lowering or increase of the predicted efficiencies.
[21] J. J. M. Halls, J. Cornil, D. A. dos Santos, R. Silbey, D.-H. Hwang, A. B. Holmes, J. L. Brédas, R. H. Friend, *Phys. Rev. B* **1999**, *60*, 5721.
[22] J. L. Brédas, D. Beljonne, V. Coropceanu, J. Cornil, *Chem. Rev.* **2004**, *104*, 4971.
[23] D. Veldman, J. J. A. M. Bastiaansen, B. M. W. Langeveld-Voss, J. Sweelssen, M. M. Koetse, S. C. J. Meskers, R. A. J. Janssen, *Thin Solid Films* **2006**, *511–512*, 581.
[24] A. J. Moulé, A. Tsami, T. W. Bünnagel, M. Forster, N. M. Kronenberg, M. Scharber, M. Koppe, M. Morana, C. J. Brabec, K. Meerholz, U. Scherf, *Chem. Mater.* **2008**, *20*, 4045.

[25] S. Xiao, H. Zhou, W. You, *Macromolecules* **2008**, *41*, 5688.
[26] J. Hou, T. L. Chen, S. Zhang, H.-Y. Chen, Y. Yang, *J. Phys. Chem. C* **2009**, *113*, 1601.
[27] M. M. Wienk, M. G. R. Turbiez, M. P. Struijk, M. Fonrodona, R. A. J. Janssen, *Appl. Phys. Lett.* **2006**, *88*, 153511.
[28] B. P. Karsten, R. A. J. Janssen, *Org. Lett.* **2008**, *10*, 3513.
[29] L. Wen, B. C. Duck, P. C. Dastoor, S. C. Rasmussen, *Macromolecules* **2008**, *41*, 4576.
[30] P. Schilinsky, U. Asawapirom, U. Scherf, M. Biele, C. J. Brabec, *Chem. Mater.* **2005**, *17*, 2175.
[31] A. M. Ballantyne, L. Chen, J. Dane, T. Hammant, M. F. Braun, M. Heeney, W. Duffy, I. McCulloch, D. D. C. Bradley, J. Nelson, *Adv. Funct. Mater.* **2008**, *18*, 2373.
[32] J. Peet, N. S. Cho, S. K. Lee, G. C. Bazan, *Macromolecules* **2008**, *41*, 8655.
[33] J. K. Lee, W. L. Ma, C. J. Brabec, J. Yuen, J. S. Moon, J. Y. Kim, K. Lee, G. C. Bazan, A. J. Heeger, *J. Am. Chem. Soc.* **2008**, *130*, 3619.
[34] D. Veldman, S. C. J. Meskers, R. A. J. Janssen, *Adv. Funct. Mater*, **2009**, *19*, 1939.
[35] K. Vandewal, A. Gadisa, W. D. Oosterbaan, S. Bertho, F. Banishoeib, I. van Severen, L. Lutsen, T. J. Cleij, D. Vanderzande, J. V. Manca, *Adv. Funct. Mater.* **2008**, *18*, 2064.
[36] M. Lenes, M. Morana, C. J. Brabec, P. W. M. Blom, *Adv. Funct. Mater.* **2009**, *19*, 1106.
[37] M. Morana, M. Wegscheider, A. Bonanni, N. Kopidakis, S. Shaheen, M. Scharber, Z. Zhu, D. Waller, R. Gaudiana, C. Brabec, *Adv. Funct. Mater.* **2008**, *18*, 1757.
[38] J. K. Lee, W. L. Ma, C. J. Brabec, J. Yuen, J. S. Moon, J. Y. Kim, K. Lee, G. C. Bazan, A. J. Heeger, *J. Am. Chem. Soc.* **2008**, *130*, 3619.